Thermomechanical modeling of glass cooling including thermal radiation using P1 method

Kossiga Agboka[a]*, Fabien Béchet[a], Philippe Moreau[a], Dominique Lochegnies[a]

a. UVHC, LAMIH, F-59313 Valenciennes, France
* Corresponding author
Email address: kossiga.agboka@univ-valenciennes.fr

ABSTRACT

Glass tempering consists in heating a glass product over its transition temperature followed by a rapid cooling to the ambient temperature. This process is used to improve the mechanical resistance of the glass product with compressive stresses on the surface and tensile stresses in the core. The mechanical behavior is very dependent on the temperature, therefore an accurate knowledge of the heat transfer during the cooling process is highly necessary to obtain the best estimation of the residual stresses. Since glass is a semi-transparent material, thermal radiation takes place in addition to the conductive heat transfer especially at high temperatures. In this paper, we performed an axisymmetric modeling of glass tempering for a circular disk in contact with a metal mold including radiative effects computed by the P1 method and compared the thermal and mechanical results to experimental measurements. Good agreements with the experimental results are obtained.

Keywords

Glass tempering, thermal radiation, residual stresses

1 Introduction

During industrial processes, glass is necessarily cooled. This more or less fast cooling leads to residual stresses in the glass products. One may want to have no residual stresses in order to have further operations on the product (like cutting) or oppositely to have residual stresses. Quenched glass products are more resistant and are used for security purposes because when fracture occurs, it leads to small pieces with blunt edges which are harmless for the user. The tempering process contributes to improve the mechanical behavior which is temperature dependent. Therefore, it is necessary to have an accurate knowledge of the heat transfer occurring during the cooling process.

As glass is a semi-transparent material which means thermal radiation is simultaneously emitted and reabsorbed inside the glass for wavelength of the semitransparent domain, radiative effects should be taken into account during the cooling process especially at high temperatures. This is done by solving the radiative transfer equation (RTE). The RTE is so complex that different methods [1], [2] are developed to solve it. Some of these method are discrete ordinate method (DOM)[3]–[5], Monte Carlo method[6], [7], finite volume method, P_N approximation method.

In this paper, we developed thermomechanical models of a glass disk supported by a metal mold using the P1 method to compute the radiative effects. Experimental measurements were performed to compare both experimental and numerical results and investigate the influence of thermal radiation on the heat transfer and the mechanical behavior.

2 Conductive and radiative heat transfer modeling

In this paper, a glass tempering model including thermal radiation was developed. A glass disk in contact with a metal mold (Figure 1) is naturally cooled from a given initial temperature. The numerical results were compared to experimental results. The finite element model is axisymmetric.

The glass domain modeled (Figure 1) is defined as: $\vec{r} = (r, z) \in D_g$ and $D_g = \{0 \leq r \leq R, 0 \leq z \leq e\}$. The mold domain is given by: $\vec{r} = (r, z) \in D_m$, $D_m = \{R_1 \leq r \leq R_2, -E \leq z \leq 0\}$. The glass and the mold surface are denoted ∂D_g and ∂D_m respectively. Since glass cooling occurs over time t between 0 and t_{max}, we defined D_g^t as the domain occupied by the glass over time which is given by: $D_g^t = D_g \times \{0 \leq t \leq t_{max}\}$. The glass surface over time is denoted ∂D_g^t and the contact zone ∂D_{gm}^t

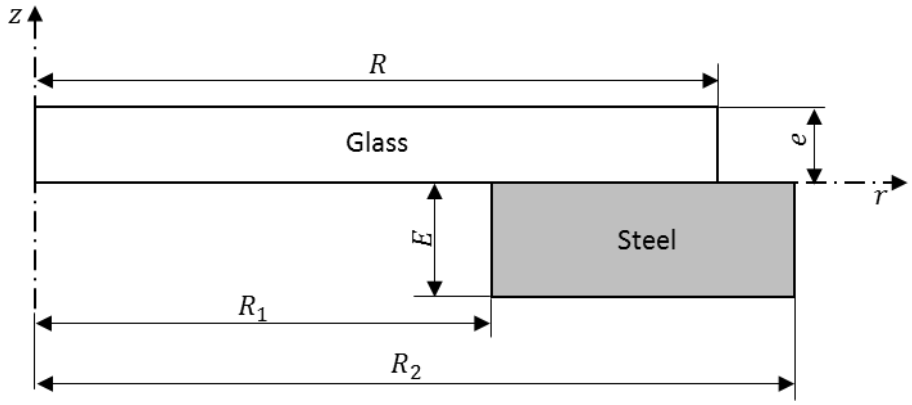

Figure 1 : Axisymmetric description of the model

The heat transfer that occurs during the cooling process of the glass disk is described by the heat equation in cylindrical coordinates:

$$c_p^g \rho^g \frac{\partial T^g(\vec{r},t)}{\partial t} = \vec{\nabla}_{\vec{r}} \cdot \left(k_h^g \vec{\nabla}_{\vec{r}} T^g(\vec{r},t)\right) - \vec{\nabla}_{\vec{r}} \cdot \vec{q}_{rad}(T^g), \qquad (\vec{r},t) \in D_g^t \tag{1}$$

$$T^g(\vec{r},0) = T_0^g(\vec{r}), \qquad \vec{r} \in D_g$$

The subscrpit « g » is related to the glass. k_h is the heat conductivity of the glass, c_p the specific heat, $T(\vec{r},t)$ is the temperature depending on the position $\vec{r}$ in the glass and the time, and T_0 the initial temperature of the glass disk, $\vec{\nabla}_{\vec{r}}$ is the divergence operator in cylindrical coordinates system (r, θ, z) with θ the azimuthal coordinate. $\vec{\nabla}_{\vec{r}} \cdot \vec{q}_{rad}$ represents the divergence of the radiative heat flux $\vec{q}_{rad}$ in the semitransparent wavelength domain which depends on the temperature of the position in the glass. The boundary conditions are given by:

$$-k_h^g \frac{\partial T^g(\vec{r},t)}{\partial n^g} = \alpha(T^g(\vec{r},t) - T_\infty) + \overrightarrow{n^g} \cdot \vec{q}_{opaque}(\vec{r}, T^g), \qquad \vec{r} \in \partial D_g^t \backslash \partial D_{gm}^t \tag{2}$$

$$-k_h^g \frac{\partial T^g(\vec{r},t)}{\partial n^g} = 0, \qquad r = 0 \tag{3}$$

where $\vec{n}$ is outer normal vector of the surface ∂D_g^t of the glass domain. Equation (2) shows that the heat flux on the boundaries of the glass is composed of two terms. The first one is the convection with the surrounding air at temperature T_∞ and α is the convection coefficient. The second term is the radiative heat flux on the glass surface in the opaque wavelength region [8]–[11] given by:

$$\overrightarrow{n^g} \cdot \vec{q}_{opaque}(\vec{r}, T^g) = \pi \gamma^g \int_{opaque} \left[B_a\left(\lambda, T^g(\vec{r},t)\right) - B_a(\lambda, T^\infty)\right] d\lambda, \tag{4}$$

$$(\vec{r},t) \in \partial D_g^t \backslash \partial D_{gm}^t$$

With γ^g the hemispherical emissivity of the surface; $B\left(\lambda, T(\vec{r},t)\right)$ the Planck function depending on the wavelength λ and the temperature of the position which is expressed as:

$$B(\lambda, T) = \frac{2hc_0{}^2}{n_g{}^2 \lambda^5 \left[e^{hc_0/(n_g \lambda k_b T)} - 1\right]} \tag{5}$$

$c_0 = 2.998 \cdot 10^8\ m/s$ is the light speed in the vacuum, $h = 6.626 \cdot 10^{-34}$ J s the Planck's constant, $k_b = 1.3807 \cdot 10^{-23} J/K$ Boltzmann's constant and n_g is the glass refractive index. $B_a(\lambda, .)$ denotes, the Planck function in the vaccum (air).

For the mold part, the heat transfer equation is:

$$c_p^m \rho^m \frac{\partial T^m(\vec{r},t)}{\partial t} = \vec{\nabla}_{\vec{r}} \cdot \left(k_h^m \vec{\nabla}_{\vec{r}} T^m(\vec{r},t)\right), \qquad (\vec{r},t) \in D_m^t \tag{6}$$

$$T^m(\vec{r},0) = T_0^m(\vec{r}), \qquad \vec{r} \in D_m$$

$$-k_h^m \frac{\partial T^m(\vec{r},t)}{\partial n^m} = \alpha(T^m(\vec{r},t) - T_\infty) + \overrightarrow{n^m} \cdot \vec{q}_m(\vec{r},T^m), \qquad \vec{r} \in \partial D_m^t \backslash \partial D_{gm}^t \tag{7}$$

$$-k_h^m \frac{\partial T^m(\vec{r},t)}{\partial n^m} = 0, \qquad r = 0 \tag{8}$$

Where subscript « m » is related to the mold; T^m is the mold temperature and $\overrightarrow{n^m} \cdot \vec{q}_m$ is the radiative flux on the mold surface. As the mold is an opaque material, $\overrightarrow{n^m} \cdot \vec{q}_m$ is:

$$\overrightarrow{n^m} \cdot \vec{q}_m(\vec{r},T^m) = \gamma^m \sigma[(T^m)^4 - (T_\infty)^4], \quad \vec{r} \in \partial D_m^t \backslash \partial D_{gm}^t \tag{9}$$

With $\sigma = 5.67 \cdot 10^{-8}\ W/(m^2K^4)$, the constant of Stefan-Boltzmann.
In the contact zone, the interface flux for the glass is expressed as:

$$-k_h^g \frac{\partial T^g(\vec{r},t)}{\partial n^g} = \alpha^{gm}\left(T^g(\vec{r},t) - T^m(\vec{r},t)\right) + \overrightarrow{n^g} \cdot \vec{q}_{gm}, \qquad \vec{r} \in \partial D_{gm}^t \tag{10}$$

For the mold part, we have:

$$-k_h^m \frac{\partial T^m(\vec{r},t)}{\partial n^m} = \alpha^{gm}\left(T^m(\vec{r},t) - T^g(\vec{r},t)\right) + \overrightarrow{n^m} \cdot \vec{q}_{mg}, \qquad \vec{r} \in \partial D_{gm}^t \tag{11}$$

α^{gm} is the themal coefficient exchange between the glass and the mold; $\vec{q}_{gm}$ and $\vec{q}_{mg}$ are radiative flux vector on the glass and mold respective surfaces in the contact zone. To determine the radiative fluxes in the equation (*1*) and (11), the radiative transfer equation must be solved.

3 Radiative transfer equation (RTE)

In the semitransparent wavelength range $[0 - 5\ \mu m]$, emission and absorption of thermal radiation occur inside the glass and we assume that there is no scattering of the radiative energy. Since the absorption $\kappa(\lambda)$ coefficient depends on the wavelength, the band model is introduced by the following expression:

$$\kappa^k = \kappa(\lambda)\,; \quad \lambda_k < \lambda < \lambda_{k+1} \tag{12}$$

k is the number of the band, λ_k and λ_{k+1} are respectively the lower and upper limits of the band k. In this paper, we will use five bands presented by Viskanta *et al* [12] for soda-lime glass.

For each band k, we define $B^k(T) = \int_{\lambda_k}^{\lambda_{k+1}} B(\lambda,T)d\lambda$ the integral the Plank's function over the band. This expression is independent of λ. In this paper, we use the P1 approximation method to solve the RTE. The radiative transfer equation for the P1 approximation method in axisymmetric coordinate system using the band model is given as [1] :

$$-\vec{\nabla}_{\vec{r}} \cdot \left(\frac{1}{3\kappa^k} \vec{\nabla}_{\vec{r}} G^k(\vec{r})\right) + \kappa^k G^k(\vec{r}) = 4\pi\kappa^k B^k\left(T(\vec{r},t)\right), \vec{r} \in D_g^t \tag{13}$$

$G^k(\vec{r})$ is the incident radiation coming from all directions to the position $\vec{r}$ in the glass. The boundary conditions assuming emission and specular reflection are given by Larsen et *al* [13]:

$$\frac{1}{3\kappa^k} \vec{\nabla}_{\vec{r}} G^k(\vec{r}) \cdot \vec{n} = \frac{1 - 2r_1}{2(1 + 3r_2)}\left(4\pi B^k(T^\infty) - G^k(\vec{r})\right), \quad (\vec{r},t) \in \partial D_g^t \backslash \partial D_{gm}^t \tag{14}$$

$$\frac{1}{3\kappa^k} \vec{\nabla}_{\vec{r}} G^k(\vec{r}) \cdot \vec{n} = \frac{1 - 2r_1}{2(1 + 3r_2)}\left(4\pi B^k(T^m) - G^k(\vec{r})\right), \quad (\vec{r},t) \in \partial D_{gm}^t \tag{15}$$

where $r_1 = 0.2855742$ and $r_2 = 0.1452082$ are coefficients calculated by Klar et *al* [14] for the refractive index of glass $n = 1.46$. For more details for the calculations of r_1 and r_2, see reference [13]. For the band model, the divergence of the radiative flux in the equation (*1*) follows:

$$\vec{\nabla}_{\vec{r}} \cdot \vec{q}_{rad}(\vec{r},T) = \sum_{k=1}^{5} \kappa^k\left[4\pi B^k\left(T(\vec{r},t)\right) - G^k(\vec{r})\right] \tag{16}$$

In the contact zone, for the glass, only the surface emission in the opaque wavelength domain is considered.

$$\overrightarrow{n^g} \cdot \vec{q}_{gm} = \gamma^g \int_{opaque} \left[B_a\left(\lambda, T^g(\vec{r},t)\right) - B_a\left(\lambda, T^m(\vec{r},t)\right)\right] d\lambda\,, \qquad (\vec{r},t) \in \partial D_g^t \backslash \partial D_{gm}^t \tag{17}$$

For the mold, in addition to the surface emission in the opaque wavelength domain, we have $\sum_{k=1}^{5}\left[\frac{1-2r_1}{2(1+3r_2)}\left(G^k(\vec{r}) - 4\pi B^k(T^m)\right)\right]$ leaving the glass surface and absorbed by the mold and $\gamma^m \sum_{k=1}^{5}\left[{B_a}^k(T^m)\right]$ is emitted by the mold surface in the semitransparent domain. The total flow for the mold in the contact is then:

$$\begin{aligned}\overrightarrow{n^m} \cdot \vec{q}_{mg} = {} & \gamma^m \int_{opaque} \left[B_a\left(\lambda, T^m(\vec{r},t)\right) - B_a\left(\lambda, T^g(\vec{r},t)\right)\right] d\lambda + \gamma^m \sum_{k=1}^{5}\left[{B_a}^k(T^m)\right] \\ & - \sum_{k=1}^{5}\left[\frac{1-2r_1}{2(1+3r_2)}\left(G^k(\vec{r}) - 4\pi B^k(T^m)\right)\right], \qquad (\vec{r},t) \in \partial D_g^t \backslash \partial D_{gm}^t\end{aligned} \tag{18}$$

To solve the radiative transfer equation using the P1 approximation, a finite element method program was written with Matlab® software and the results were computed to calculate the divergence of the radiative heat flux which was then injected in Abaqus® calculation.

4 Mechanical behavior modeling

The static equilibrium of the glass disk in the absence of gravity and inertial forces in a cylindrical coordinate system is:

$$\vec{\nabla}_{\vec{r}} \cdot \bar{\bar{\sigma}}(\vec{r},t) = \vec{0}, \quad (\vec{r},t) \in D_g^t \tag{19}$$

With $\bar{\bar{\sigma}}(\vec{r},t)$ the Cauchy stress tensor; for an axisymmetric problem, equation (19) becomes:

$$\begin{cases} \dfrac{\partial \sigma_{rr}}{\partial r}(\vec{r},t) + \dfrac{\sigma_{rr}(\vec{r},t) - \sigma_{\theta\theta}(\vec{r},t)}{r} + \dfrac{\partial \sigma_{rz}}{\partial z}(\vec{r},t) = 0 \\ \dfrac{\partial \sigma_{rz}}{\partial r}(\vec{r},t) + \dfrac{\sigma_{rz}(\vec{r},t)}{r} + \dfrac{\partial \sigma_{zz}}{\partial z}(\vec{r},t) = 0 \end{cases} \tag{20}$$

The displacement vector in the glass is written as:

$$\vec{u}(\vec{r},t) = \begin{Bmatrix} u_r(\vec{r},t) \\ 0 \\ u_z(\vec{r},t) \end{Bmatrix} \tag{21}$$

For the boundary conditions, we have:

- Since the problem is axisymmetric, the radial displacement is null on the axis $r = 0$ (Figure 1)

$$u_r(\vec{r},t) = 0\,;\ (\vec{r},t) \in D_g^t, \qquad r = 0 \tag{22}$$

- The glass surface $\partial D_g^t \backslash \partial D_{gm}^t$ is free of external forces

$$\bar{\bar{\sigma}}(\vec{r},t) \cdot \vec{n} = \vec{0}, \quad (\vec{r},t) \in \partial D_g^t \backslash \partial D_{gm}^t \tag{23}$$

- On the contact interface ∂D_{gm}^t, we have a unilateral contact condition where the displacement must satisfy the Signorini condition. It states that bodies cannot interpenetrates and only contact forces exist when the distance between the bodies vanishes [15].

The stress tensor $\bar{\bar{\sigma}}(\vec{r},t)$ and the strain tensor $\bar{\bar{\varepsilon}}(\vec{r},t)$ are linked by the constitutive law.
At a given temperature, glass has a viscoelastic behavior [16]. The assumptions and the viscoelastic properties used for this model can be found in references [17], [18]

5 Experimental procedure for the glass tempering

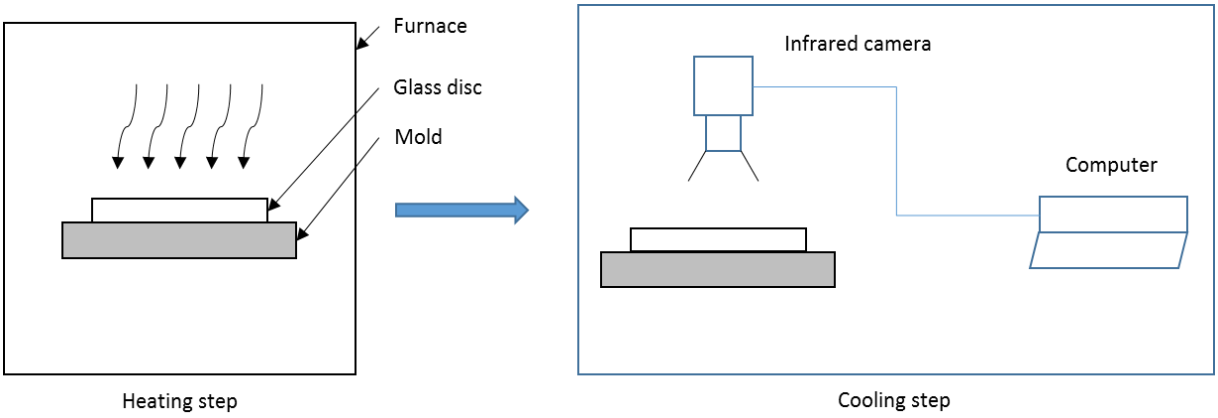

Figure 2 : Steps during the glass tempering process

In order to validate the numerical model described in the previous sections, cooling experiments were performed on glass disk. The radius of the glass disk is $R = 45$ mm and the thickness $e = 6$ mm. We used a structural steel of grade S235 for the mold. The external radius of the mold is $R_2 = 49$ mm and the thickness is $E = 8$ mm. To investigate the influence of the contact area on the thermal and mechanical behavior, we used different inner radi R_1 $(0, 15, 30, and\ 40\ mm)$ (Figure 1) for the mold. In this paper, we present just the results for $R_1 = 0\ mm$ (disk) and $R_1 = 40\ mm$ (ring).

In the first step of the tempering process, both of the glass disk and mold were heated in a furnace at 625 °C. The heating time was 2 hours in order to have a homogeneous temperature inside the glass and the mold. A thermocouple of type K was introduced in the mold at 2 mm from the upper surface to monitor the temperature during the heating step and to assume that we reached the wanted temperature.

In the second step, the glass and the mold were taken out of the furnace for the cooling process. During the cooling step, the temperature change on the top surface of the glass was recorded using an infrared camera while the mold temperature was saved with an acquisition system from Gantner Instrument. We used Optris PI450 infrared camera which has a wide temperature range from 200 to 1500 °C. Figure 2 shows the different steps of the tempering experiment.

Once, the glass and the mold temperatures reached the room temperature, the glass sample was observed with a circular polariscope to visualize the distribution of the phase retardation induced by the residual stresses state in the glass.

6 Input data for the model

The dimensions of the glass disk and the mold modeled were the same as in section 5 in order to compare the numerical results to the experimental data. The experiment was conducted in natural convection, so the convection coefficient was taken the reference [12] and was $\alpha = 4.25\ Wm^{-2}K^{-1}$. The contact conductance was $\alpha^{gm} = 2800\ Wm^{-2}K^{-1}$ [19]. The surrounding temperature was $T_\infty = 25\ °C$ and the initial temperature was $T_0 = 625\ °C$ for both glass and mold domains.

The thermal conductivity of the glass [20] and the mold [21] were given by the following expression respectively:

$$k_h^g(T) = 1.14 + 0.000624T \tag{24}$$

$$k_h^m(T) = 54 - \frac{T}{300},\ for\ 20 < T \leq 800\ °C \tag{25}$$

The specific heat of the mold [21] is expressed as follows:

$$\begin{aligned} c_p^m(T) &= 425 + 0.733T + 169 \times 10^{-6}T^2 + 2.22 \times 10^{-6}T^3,\ for\ 20 \leq T \leq 600\ °C \\ c_p^m(T) &= 666\left(\frac{13002}{T - 738}\right),\ for\ 600 < T \leq 735\ °C \end{aligned} \tag{26}$$

Where T is in $°C$. The glass one was taken from [20]. The densities of the glass and the mold were respectively $2500\ kg/m^3$ and $7850\ kg/m^3$. Glass and mold emissivity were taken from [9].

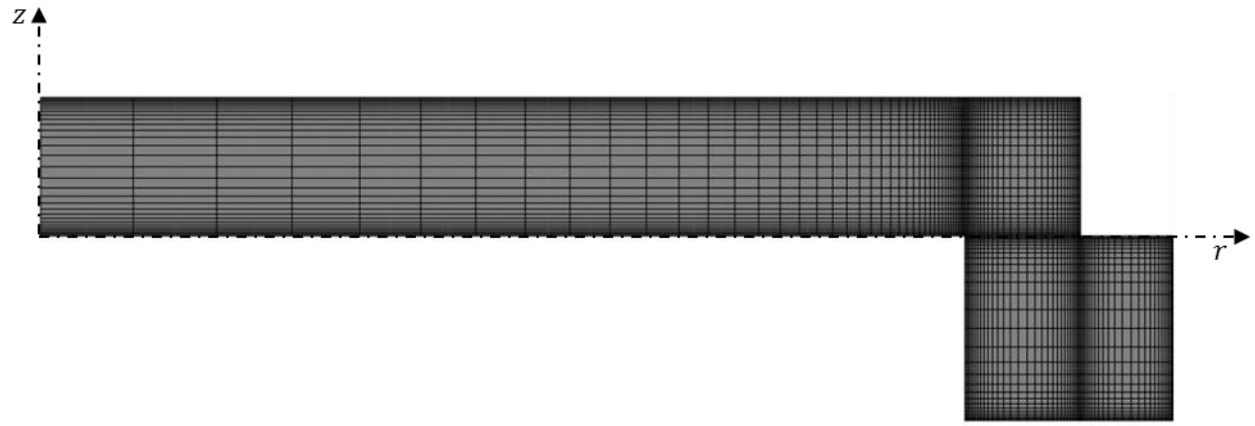

Figure 3 : Meshing of the model

The thermomechanical model was solved using Abaqus® software. The glass and the mold domains were meshed such a way to avoid mesh dependent results. The mesh was also refined near the surfaces and the contact zones (Figure 3) in order to have an accurate estimation of the temperature gradient due to the convective and radiative effects and also an accurate computation of the incident radiation which has high gradient at the surface vicinity. CAX8T elements with biquadratic interpolation for displacement and bilinear interpolation for temperature were used to solve mechanical and thermal equations. For each time increment, the RTE was solved using the same mesh in the glass and the divergence of the radiative flux computed was injected in the Abaqus® calculation via a subroutine written in FORTRAN.

7 Results and discussion

7.1 Temperature results

In this section, results for temperature were compared to the experimental data from the cooling process exposed in the section 5. The thermomechanical model presented before was performed and coupled with the P1 method to compute the radiative effects. To investigate the influence of the thermal radiation on the heat transfer, a model taking into account only conductive heat transfer and another one with surface radiation on the boundaries of the mold and the glass were performed. The model without thermal radiation was noted "Norad" and the second one was called "Rad".

The comparison of the numerical results to the experimental data for the glass supported by the mold with $R_1 = 0\ mm$ was shown in the Figure 4 on one hand and on the other hand, the one for the glass supported by the mold with $R_1 = 40\ mm$ in the Figure 5. For both figures, the temperature change was plotted for the point $(0, e)$.

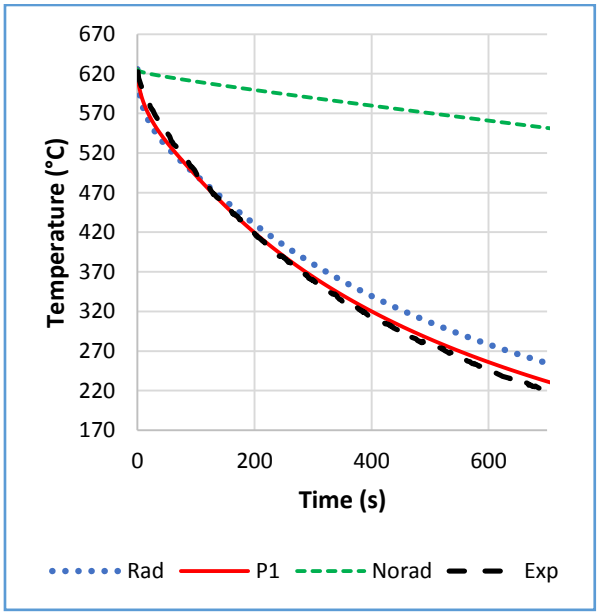

Figure 4 : Temperature in the center of the upper surface of the glass tempered with the mold of $R_1 = 0\ mm$

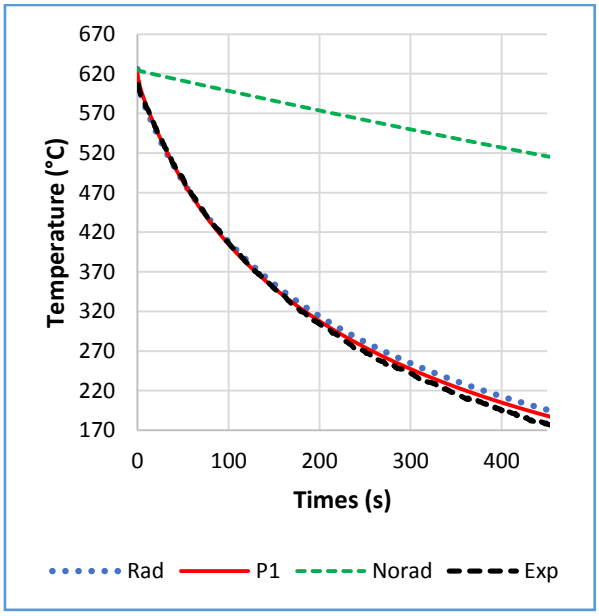

Figure 5 : Temperature in the center of the upper surface of the glass tempered with the mold of $R_1 = 40\ mm$

Figure 4 and Figure 5 show a great difference between the model the experimental results and the numerical one for the model without thermal radiation effects while a good aggreement can be observed with the model with the surface radiationand the one coupling the radiative effects computed by the P1 method. Computing the radiative effects inside the glass brings a better accuracy in the numerical results. The cooling rate of the glass was affected by the contact area ∂D_{gm}^{t}. The temperature of the glass supported by the mold $R_1 = 0\ mm$ reached $220\ °C$ after $600\ s$. The glass disk in contact with the mold ring of $R_1 = 40\ mm$ had its temperature under $220\ °C$ after $350\ s$. This results from the fact a small surface of the glass is in contact with the hot mold leading to a higher surface cooled by natural convection. The cooling rate gets high when the contact zone is small.

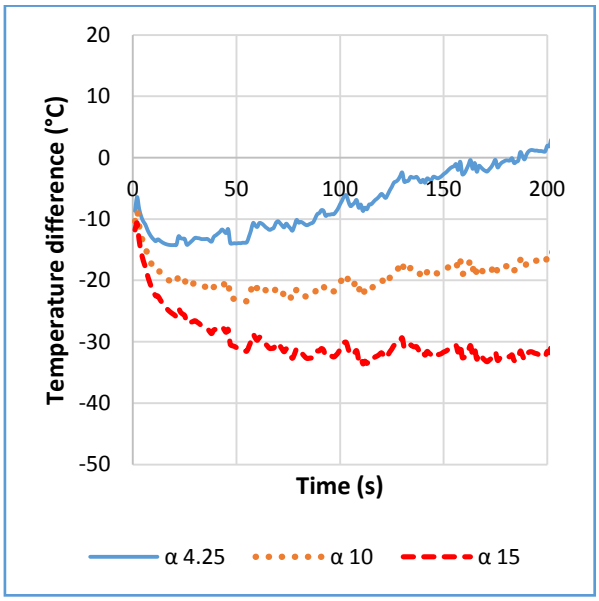

Figure 6 : Temperature difference between the simulaion and the experimental data for different convection coefficient (disk)

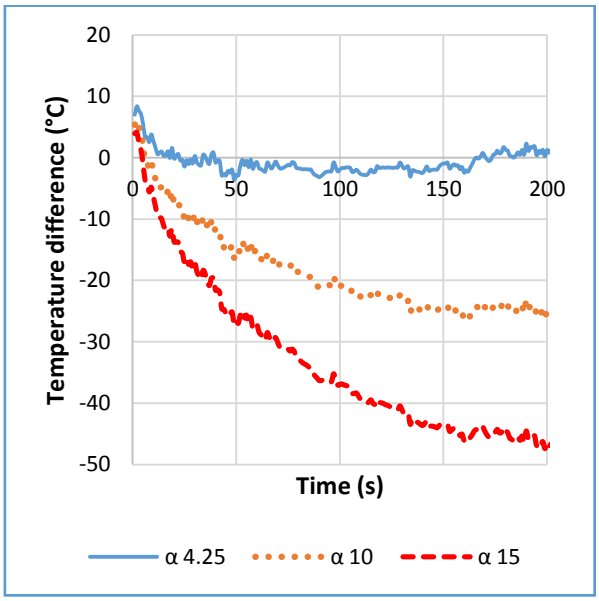

Figure 7 : Temperature difference between the simulaion and the experimental data for different convection coefficient (Ring)

To investigate the sensibility of the convection coefficient value on the numerical results, additional calculations were performed for the value of $\alpha = 10\ and\ 15\ Wm^{-2}K^{-1}$. Figure 6 and Figure 7 show the temperature difference between the experimental data and the numerical results for the glass cooled with repectively with the disk and the ring molds. The temperature difference increases with the convection coefficient. For the disk mold case (Figure 6), the maximum temperature error is about 30°C (7% of relative error) for $\alpha = 15\ Wm^{-2}K^{-1}$ in 200 s whereas the ring case (Figure 7) shows about 50 °C (15% of relative error). The convection coefficient $\alpha = 4.25\ Wm^{-2}K^{-1}$ has the lowest errors (2.56 % for the disk and 1.39 % for the ring) with the experimental data.

7.2 Stress results

When glass is cooled, a layer near the surfaces is classically submitted to compressive stresses and the core to tensile stresses [22]. This can be observed in Figure 8 where is shown the distribution of the circumferential stress $\sigma_{\theta\theta}$ in the glass. Due to the presence the hot mold, the contact surface ∂D_{gm}^{t} is not submitted to compressive stresses.

Figure 8: Circumferential residual stress distribution in the glass supported by the mold ring of $R_1 = 40\ mm$

The stress distribution through the thickness of a tempered glass is parabolic with compression in the surface layers and tension in the core. Figure 9 presents the evolution of residual stresses through the thickness on the axis for the glass in contact with both types of mold (disk and ring).

In the case of the disk mold, tensile residual stresses are observed through the whole thickness along the axis even in the surface layers. The glass receives heat from the mold at its lower surface. This reduces the cooling rate in the glass and the surface layers are not cooled fast enough to have compressive residual stresses. The tensile stresses reached $10\ MPa$ in the core and less than $5\ MPa$ in the surface layers. It is better to have compressive stresses in the surface because compression closes small cracks at the surface improving then the mechanical behavior of the glass.

In the case of the glass cooled with the mold of inner radius $R_1 = 40\ mm$ (ring), the surfaces are effectively in compression. This is due to the absence contact with the mold near the center of the glass disk leading to a higher cooling rate by convection. The compressive stresses are about $-17\ MPa$ at the surface while the core is submitted to tension of $7\ MPa$. To increase the stress level, forced convection should be used.

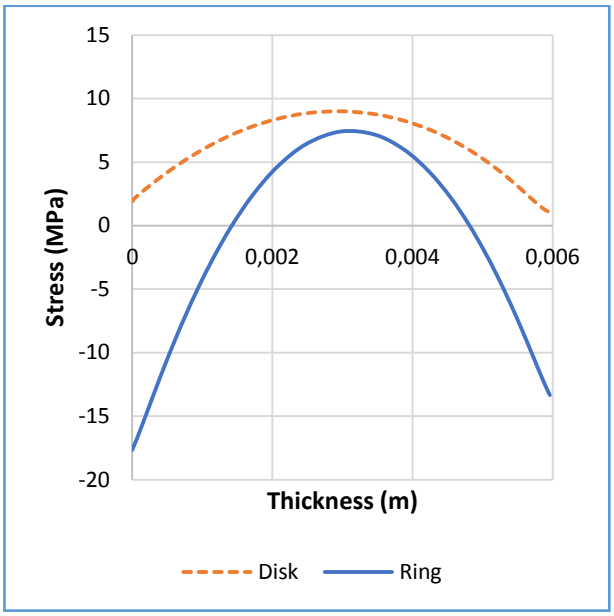

Figure 9 : Circumferential residual stress ditribution along the thickness in the glass on the axis for the P1 method

7.3 Comparison with the photoelasticity observations with a polariscope

After the cooling of the glass disks to the room temperature, the samples were observed with a circular polariscope. The principle is to propagate a polarized light through the glass in a direction. The light leaving the glass vibrates according to the principal stresses contained in the plane perpendicular to the direction of propagation of the light. In our case the propagation direction is along the revolution axis of the glass disk.

The phase delay between the principal directions contained in the plane of glass disk is given by [23]:

$$\Delta = C \int_0^e (\sigma_1 - \sigma_2) dz \qquad (27)$$

Where σ_1 and σ_2 are the principal stresses in the plane of the glass disk in cartesian coordinates system; $C = 2.6\ TPa^{-1}$ the photoelastic constant of the glass.

In order to compare the observations of the stress distribution in the glass to the numerical results, a program was written to compute the phase delay using the stress results from the thermomechanical model coupled with P1 method. The axisymmetric stress tensor was brought to the Cartesian coordinates system by rotation, then a numerical integration was performed using trapeze method to calculate Δ. The comparisons are shown in Figure 10 and Figure 11 respectively for glass tempered with mold of inner radius $R_1 = 0\ mm$ and $R_1 = 40\ mm$.

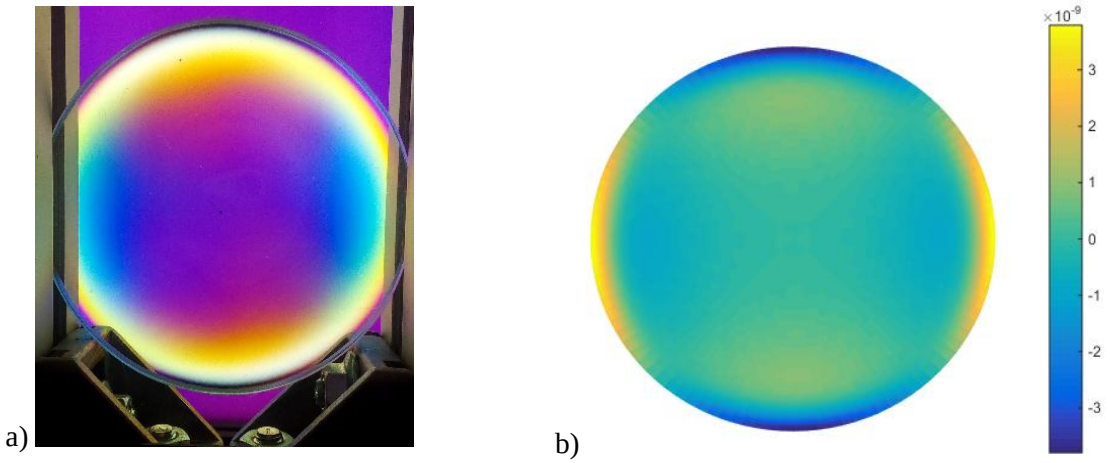

Figure 10 :Comparison of the phase retardation between (a) experimental observations and (b) calculation for the disk mold

a)  b) 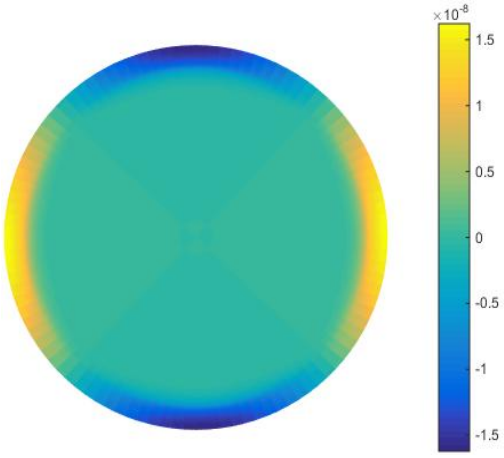

Figure 11 : Comparison of the phase retardation between (a) experimental observations and (b) calculation for the ring

The calculated distribution of the phase delay induced by the stress state in the glass is in good agreement with the experimental observations. In the case of the Figure 11, the phase delay is almost null inside the zone of the glass disk without contact with the mold ring. This means that the difference $\sigma_1 - \sigma_2 = 0$ leading to an isotropic stress state in the plane of the glass disk. The difference between the principal stresses in the same plane is not null for the contact zone. For Figure 10, the absolute value of the phase delay decreases from the boarder to the center of the glass disk. An anisotropic stress state inside the glass can be noticed due to the full contact of the lower surface with the mold.

Conclusion

This paper deals with thermomechanical modeling of the tempering process of a circular glass disk supported by a metal mold by taking into account radiative effects computed by the P1 method and experimental investigation of the tempering process.

The comparison between experimental and numerical results shows that thermal radiation takes a great importance for the heat transfer during the cooling process in natural convection. It can be seen that the P1 method describes quite well the temperature change of the glass; however, one should note that it is known to be a diffusive method and can affect the prediction of the stress level. The contact area also has an influence on the heat transfer. Bigger is the contact zone, more it affects the cooling rate.

The prediction of the distribution of the phase delay induced by the stress state in the glass has good agreement with the experimental observations. An anisotropic stress state in the glass was observed in the contact zone. To avoid this anisotropic state, the contact area must be as small as possible. The high temperature of the mold leads to low stress levels in the glass; therefore experiments with cold mold should be performed to have a more realistic stress level compared to industrial processes.

References

[1] M. F. Modest, *Radiative heat transfer*. Academic press, 2013.

[2] J. R. Howell, M. P. Menguc, et R. Siegel, *Thermal Radiation Heat Transfer, 5th Edition*. CRC Press, 2010.

[3] W. A. Fiveland, « Discrete-Ordinates Solutions of the Radiative Transport Equation for Rectangular Enclosures », *J. Heat Transf.*, vol. 106, n° 4, p. 699‑706, nov. 1984.

[4] J. S. Truelove, « Discrete-Ordinate Solutions of the Radiation Transport Equation », *J. Heat Transf.*, vol. 109, n° 4, p. 1048‑1051, nov. 1987.

[5] K. D. Lathrop, « Use of Discrete-Ordinates Methods for Solution of Photon Transport Problems », *Nucl. Sci. Eng.*, vol. 24, n° 4, p. 381‑388, avr. 1966.

[6] N. V. Nikonorov, A. K. Przhevuskii, et A. V. Chukharev, « Characterization of non-linear upconversion quenching in Er-doped glasses: modeling and experiment », *J. Non-Cryst. Solids*, vol. 324, n° 1‑2, p. 92‑108, août 2003.

[7] W. Zhou et T. Qiu, « Zone modeling of radiative heat transfer in industrial furnaces using adjusted Monte-Carlo integral method for direct exchange area calculation », *Appl. Therm. Eng.*, vol. 81, p. 161‑ 167, avr. 2015.
[8] K. H. Lee et R. Viskanta, « Transient conductive-radiative cooling of an optical quality glass disk », *Int. J. Heat Mass Transf.*, vol. 41, n° 14, p. 2083‑ 2096, juillet 1998.
[9] N. Siedow, D. Lochegnies, F. Béchet, P. Moreau, H. Wakatsuki, et N. Inoue, « Axisymmetric modeling of the thermal cooling, including radiation, of a circular glass disk », *Int. J. Heat Mass Transf.*, vol. 89, p. 414‑ 424, oct. 2015.
[10] F. Béchet, N. Siedow, et D. Lochegnies, « Two-dimensional finite element modeling of glass forming and tempering processes, including radiative effects », *Finite Elem. Anal. Des.*, vol. 94, p. 16‑ 23, févr. 2015.
[11] H. Loch et D. Krause, Éd., « Mathematical Simulation in Glass Technology », in *Mathematical Simulation in Glass Technology*, Berlin, Heidelberg: Springer Berlin Heidelberg, 2002.
[12] R. E. Field et R. Viskanta, « Measurement and Prediction of the Dynamic Temperature Distributions in Soda-Lime Glass Plates », *J. Am. Ceram. Soc.*, vol. 73, n° 7, p. 2047–2053, 1990.
[13] E. W. Larsen, G. Thömmes, A. Klar, M. Seaïd, et T. Götz, « Simplified PN Approximations to the Equations of Radiative Heat Transfer and Applications », *J. Comput. Phys.*, vol. 183, n° 2, p. 652‑ 675, déc. 2002.
[14] A. Klar, J. Lang, et M. Seaïd, « Adaptive solutions of -approximations to radiative heat transfer in glass », *Int. J. Therm. Sci.*, vol. 44, n° 11, p. 1013‑ 1023, nov. 2005.
[15] P. Wriggers, *Computational contact mechanics: with 12 tables*, 2. ed. Berlin: Springer, 2006.
[16] A. Q. Tool et J. Valasek, *Concerning the annealing and characteristics of glass*. Govt. Print. Off., 1920.
[17] L. Daudeville et H. Carre, « Thermal tempering simulation of glass plates: inner and edge residual stresses », *J. Therm. Stress.*, vol. 21, n° 6, p. 667–689, 1998.
[18] J. H. Nielsen, J. F. Olesen, P. N. Poulsen, et H. Stang, « Finite element implementation of a glass tempering model in three dimensions », *Comput. Struct.*, vol. 88, n° 17–18, p. 963‑ 972, sept. 2010.
[19] A. Y. Yi et A. Jain, « Compression Molding of Aspherical Glass Lenses–A Combined Experimental and Numerical Analysis », *J. Am. Ceram. Soc.*, vol. 88, n° 3, p. 579‑ 586, mars 2005.
[20] D. Mann, R. E. Field, et R. Viskanta, « Determination of specific heat and true thermal conductivity of glass from dynamic temperature data », *Wärme- Stoffübertrag.*, vol. 27, n° 4, p. 225–231, 1992.
[21] V. A. Narang, « Heat transfer analysis in steel structures », Worcester Polytechnic Institute, 2005.
[22] D. Uhlmann, *Elasticity and Strength in Glasses: Glass: Science and Technology*. Elsevier, 2012.
[23] G. L. Cloud, *Optical methods of engineering analysis*. Cambridge: Univ. Press, 1995.